The AAPM/RSNA Physics Tutorial for Residents

CME FEATURE

This article meets the criteria for 1.0 credit hour in Category 1 of the AMA Physician's Redognition Award. To obtain credit, see the questionnaire on pp 919–922.

Introduction to Emission CT[1]

Mark T. Madsen, PhD

The article explores the fundamentals of emission computed tomography (CT) from a nonmathematical approach. Tomographic images reveal the internal distributions of radioactivity in three-dimensional objects, and thus allows anatomic localization and improves contrast. Tomography requires a stable distribution of radionuclides, uniform detector response, an accurate center of rotation, and a complete set of projections. In emission CT, a large number of measurements, called projections, are collected at various angles about the patient during the examination. This information is organized by the angles of acquisition into a stack, called a sinogram. Each projection is modified by applying a reconstruction filter (eg, ramp or windowed reconstruction filters). These modified projections are backprojected to form the transverse tomographic images. The quality of tomographic images generated from filtered backprojection depends on the underlying assumptions about the projections. Typical artifacts that result from violations of these assumptions include motion, uniformity, and attenuation artifacts. In addition, an inaccurate center of rotation, insufficient angular sampling, and errors in selection of pixel size can result in poor-quality reconstructed images.

■ INTRODUCTION

In a wide variety of scientific and imaging disciplines, the following question has frequently appeared: "Is it possible to determine the internal distribution of a three-dimensional object solely from external measurements?" The answer to this question is a qualified "yes." It is possible if the external measurements constitute a complete set of projections. The key words are complete and projections because they encompass all of the basic assumptions on which all computed tomography (CT) depends. This is especially true for emission CT, in which the tomographic images reflect the distribution of radioactivity within a patient.

This article is a nonmathematical presentation of the basics of emission CT. In it, the mechanics of image reconstruction are examined, and single photon emission computed tomography (SPECT) and positron emission tomography (PET), the two modali-

Abbreviations: FWHM = full-width-at-half-maximum, HMPAO = hexamethyl-propyleneamine oxime, PET = positron emission tomography, SPECT = single photon emission computed tomography

Index terms: Emission CT (ECT) • Images, artifact • Images, processing • Physics

RadioGraphics 1995; 15:975–991

[1] From the Department of Radiology, University of Iowa, 200 Hawkins Dr, Iowa City, IA 52242. From the AAPM/RSNA Physics Tutorial at the 1994 RSNA scientific assembly. Received February 15, 1995; revision requested April 19 and received May 6; accepted May 9. **Address reprint requests to** the author.

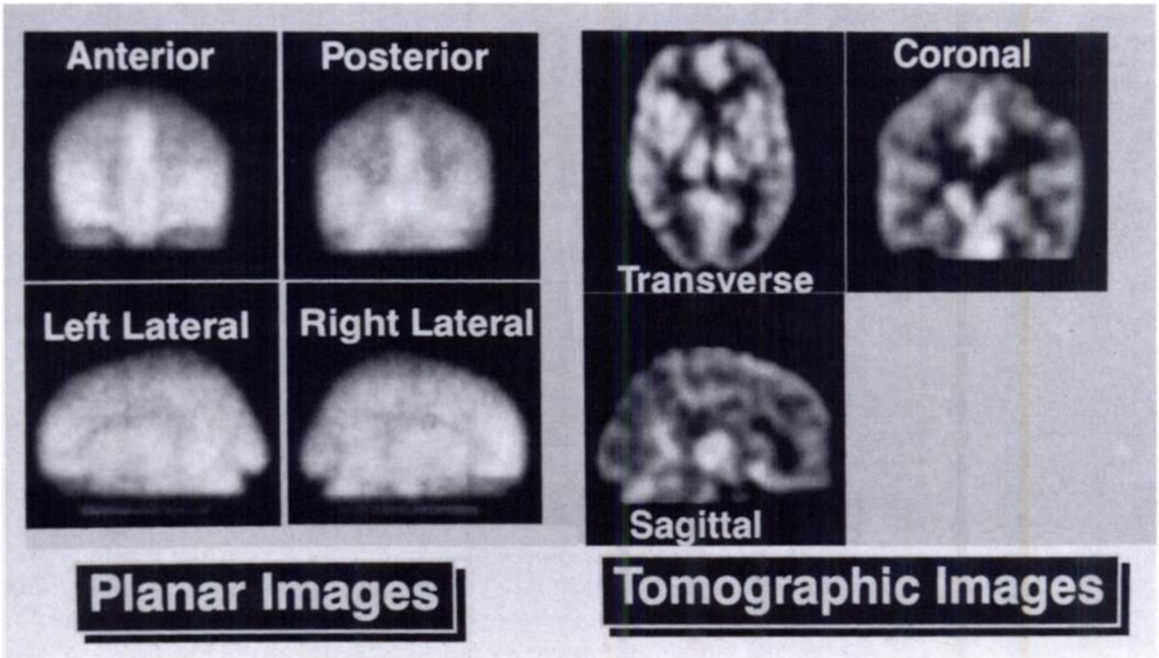

Figure 1. Planar images versus emission CT images. On conventional planar images from a technetium-99m hexamethyl-propyleneamine oxime (HMPAO) brain perfusion study, depth information is compressed and internal structures are obscured because the images are two dimensional. Additional views at other viewing angles can help compensate for this problem to a small degree. In comparison, tomographic views of the same distribution provide high-contrast displays of the internally distributed radionuclides.

ties that constitute emission CT, are briefly described. The concepts of projections, backprojection, filtered backprojection, and reconstruction filtering are defined and examined within the limits imposed by SPECT and PET instrumentation. In addition, the basic assumptions of emission CT are analyzed and examples of common artifacts are given. Although mathematics has been eliminated from the description of tomography to foster understanding, this omission imposes limitations. The interested reader is strongly encouraged to consult the references for a more thorough treatment of emission CT (1-8).

■ OVERVIEW OF EMISSION CT

The motivation for using emission CT is simple. Tomographic sections reveal the internal distributions of radioactivity in three-dimensional objects. This additional information helps localize areas of interest accurately. Even more important, tomographic information can provide a substantial gain in contrast. Contrast is a measure of the count density in an area of interest in an image with respect to the count density in the surrounding structures. In nontomographic planar imaging (scintigraphy), contrast is often low because of radioactivity in front of and behind the area of interest. Emission CT removes this superimposition, thus vastly improving the detectability of abnormal areas. However, this added information does not come free. Emission CT requires more expensive equipment and more stringent quality control than does conventional scintigraphy. In addition, it is also more susceptible to artifacts.

The advantages of emission CT are illustrated in Figure 1. Although the conventional scintigrams provide some diagnostic information, not much can be deduced about internal structures. In the emission CT views, the internal structures are clearly visible. This information also gives visual cues that help the observer associate the anatomy with the image data. These tomographic views were reconstructed from 90 planar views acquired at 4° increments about the patient's head. All of the images in this article are digital; that is, they are a matrix of numbers that have been gray-scale coded for display. The matrix values correspond to the distribution of radioactivity in the object being imaged. The matrix size is generally 128 × 128 (although both 64 × 64 and 256 × 256 matrices are occasionally used), and the size of a matrix element (pixel) is usually 2-6 mm.

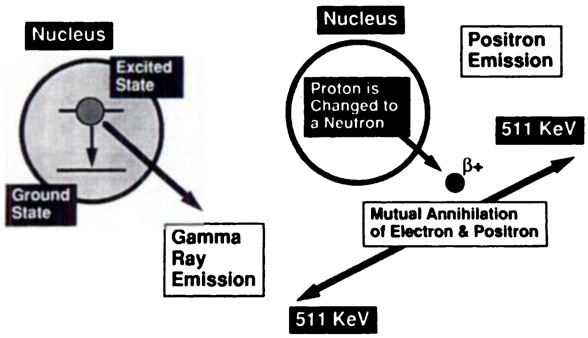

2.

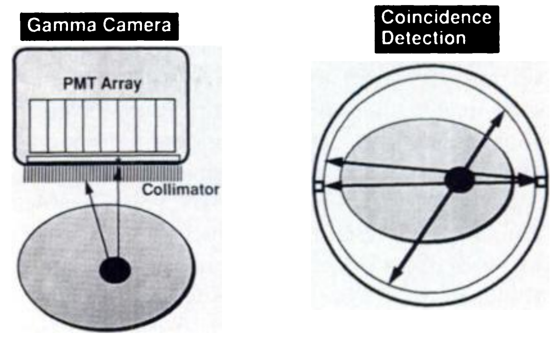

3.

Figures 2, 3. **(2)** Diagrams of SPECT and PET radionuclides. Radionuclides used in emission CT decay with the emission of a gamma ray (SPECT) or the emission of a positron (PET). In SPECT studies, the gamma rays are detected, and in PET studies, it is the 511 keV annihilation photons that are detected. **(3)** Diagrams of emission CT detection schemes. Gamma cameras acquire information in SPECT studies by using collimators as the image-forming apertures. Collimators have a very low sensitivity. PET cameras use coincidence imaging to collect the data used to reconstruct tomographic images.

Table 1
Radionuclides Commonly Used in SPECT

Radionuclide	Half Life	Photon Energy (keV)
Technetium-99m	6 h	140
Iodine-123	13 h	159
Indium-111	67 h	172, 247
Thallium-201	73 h	60–80*, 167
Gallium-67	78 h	93, 185, 300
Iodine-131	8 d	364

*Mercury x rays.

Emission CT can be separated into two distinct categories: SPECT, which uses conventional nuclear medicine radionuclides and imaging devices such as the gamma camera, and PET, which uses only positron-emitting radionuclides and coincidence detection. Both modes of imaging have several common features that impose limitations on the quality of the tomographic images. In each case, the emitted photons from the internal radionuclide distributions can be absorbed or scattered within the patient (attenuation). In addition, statistical fluctuations (referred to as noise) are a fundamental, unavoidable part of the emission and detection of radiation.

• Single Photon Emission Computed Tomography

In SPECT studies, gamma rays emitted from the patient are detected and mapped into an image. Often during the process of radioactive decay, the nucleus is in an excited energy state, and it may emit a high-energy photon (gamma ray) as it returns to its lowest energy state (Fig 2). The gamma ray energies encountered in scintigraphy range from 80 to 364 keV (Table 1), with the 140 keV gamma ray of Tc-99m being the most common. Despite attenuation, a sufficient number of gamma rays will be transmitted from their origin within the body to an external detector such as a gamma camera.

A gamma or scintillation camera generates a two-dimensional image of the radionuclide distribution (Fig 3). The sensitive element of the system is a large, thin, sodium iodide crystal that converts the absorbed gamma ray energy into visible light (ie, a scintillation). This light flash is sensed by an array of photomultiplier tubes, which allow the position of the interaction on the crystal to be determined. The imaging aperture of the gamma camera is a lead plate with multiple holes called a collimator. The collimator projects the internal source distribution onto the sodium iodide crystal by passing gamma rays with a specific trajectory. All other gamma rays are absorbed. This method of imaging is very inefficient because less than one of 2,000 gamma rays that reach the collimator are transmitted through to the sodium iodide crystal.

SPECT systems collect the necessary external emission data from one or more gamma cameras mounted on a gantry, which rotates about a pallet supporting the patient. The gamma cameras also can translate in and out in the radial direction to maintain proximity to the patient during the data collection. Sixty to 120 separate views are acquired over a 180° or 360° rotation. The field of view of the gamma camera is typically 40–50 cm across the patient and 30–40 cm in the axial direction.

Values of spatial resolution for a SPECT system range from 8 mm for high-count studies of the brain to greater than 20 mm for low-count studies of the torso. The imaging time for a single SPECT study is typically 15–30 minutes (2,9).

• Positron Emission Tomography

PET systems use radionuclides that decay with the emission of a positron (Fig 2). The positron is the antiparticle of the electron; when the positron and electron meet, mutual annihilation occurs, with the emission of two collinear 511-keV photons. This feature of positron decay allows the localization of a positron source by means of coincidence detection, in which opposed detectors must absorb both of the annihilation gamma rays.

A PET imaging system consists of multiple coincidence detectors surrounding the patient, which obviates the use of lead collimators. The elimination of collimators gives the PET system its resolution and sensitivity advantages over a SPECT system. The other major advantage associated with use of positron emitters is that they include many physiologically important elements, such as carbon, nitrogen, and oxygen (Table 2).

PET systems come in a wide variety of designs, but all use coincidence detection instead of lead collimators to collect the projection data used to produce tomographic images (Fig 3). One popular design uses a large array of individual detectors that totally surround the patient. Because of the large number of detectors and coincidence imaging, all of the measurements can be acquired without motion of the gantry. The gantry bore is 55 cm in diameter to accommodate the body trunk, and the axial field of view is 10–15 cm.

The spatial resolution of a PET system is about 5–10 mm, and it is about 30–100 times more sensitive than a SPECT system. The imaging time for a PET study can be as short as 5 seconds, but it is often in the range of 1–10 minutes (2,10,11).

Table 2
Radionuclides Commonly Used in PET

Radionuclide	Half Life	Photon Energy (keV)
Oxygen-15	2 min	511
Carbon-11	20 min	511
Nitrogen-13	10 min	511
Fluorine-18	110 min	511
Rubidium-82	75 sec	511

■ FUNDAMENTAL ASSUMPTIONS OF EMISSION CT

The steps required for emission CT as it is performed in most clinics can be summarized briefly. A large number of measurements referred to as projections are collected at various angles about the patient during the SPECT or PET study. This information is organized by the angles of acquisition into a stack, often referred to as a sinogram. Each of these projections is modified by a reconstruction filter, and these modified projections are backprojected to form the transverse tomographic images. As with all tomography, emission CT is a mathematical construct based on (and thereby limited by) several underlying assumptions: (*a*) The distribution of radionuclides is both spatially and temporally static, (*b*) the sensitivity of the detectors collecting the external measurements is uniform and stable, (*c*) the center of rotation is accurately known, and (*d*) a complete set of projections is collected. Although these steps and assumptions are easily stated, a true understanding of emission CT requires a detailed examination of the basic definitions and terms.

• Projections

Tomographic imaging requires a complete set of projections. The word *projection* can have many meanings, but in tomography its definition is very specific. A projection is a set of ray sums collected at a given angle; that is, it is a set of numbers that a measuring device (such as a SPECT or PET system) collects (Fig 4). A ray sum is a single number that is the sum of all of the activity along a selected path through an object. If all of the rays are parallel to each other, the result is a parallel projection.

The projection sampling in SPECT is determined by the collimator, and most SPECT systems collect the data as parallel projections, although fan beam geometries can also be used. Projection sampling in PET has an inherent fan beam geometry because of coincidence detection (Fig 5). For simplicity and unity, a parallel

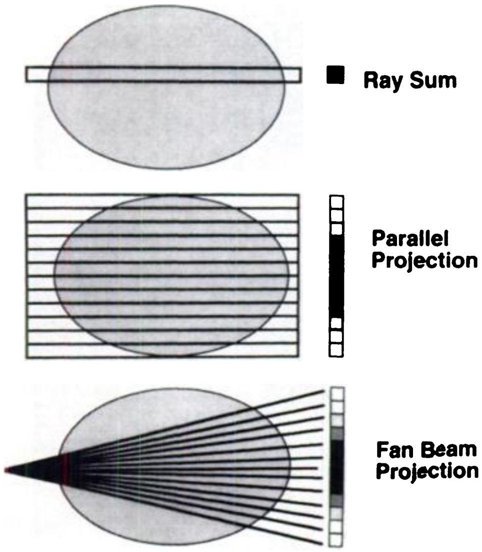

Figure 4. Diagrams illustrate some basic facts about projections. The top diagram depicts an object with an internal distribution of radioactivity (gray area) with a line through it. The sum of all of the activity along this line is a number called a ray sum. The middle diagram shows a parallel set of ray sums at one angle, referred to as a parallel projection. Projections can have other geometries such as the fan beam, which is shown in the bottom diagram.

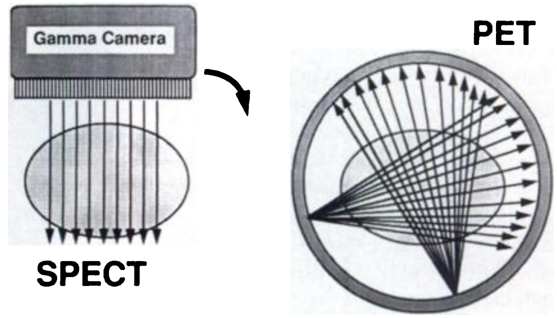

Figure 5. Diagrams of projection sampling schemes. The projection sampling scheme in SPECT (left) is determined by the collimation, which may have either a parallel or fan beam geometry. The projection sampling scheme in PET (right) is determined by the coincidence rays formed between a large number of detectors and has an inherent fan beam geometry.

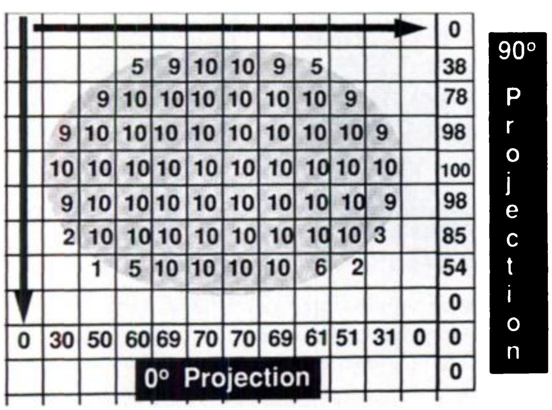

Figure 6. Projections. In the diagram, the distribution of radioactivity in the object being imaged is a constant field, with a count value of 10 in some arbitrary units at each point. The 0° projection is found by adding the count values along each column. Thus, the central value of the 0° projection is 70, since there are seven cells with a value of 10. Similarly, the 90° projection is found by adding all of the count values along each row. The central value of the 90° projection is 100, since there are 10 cells. Other projections are found by considering a set of parallel rays at other angles.

geometry is assumed in the following discussion about reconstruction; however, similar operations can also be performed for fan beam data collection.

It should be realized at the outset that neither SPECT nor PET systems directly collect the type of projection data needed for true tomography. Attenuation of the emitted gamma rays by body tissues is a major problem, since attenuation distorts the relationship between the number of detected events and the amount of activity observed. That is, the number of detected counts depends not only on the activity present but also on the length of the path that the photon travels through the body tissues before it reaches the detector. Other factors that also affect the quality of tomographic images include statistical fluctuations in the measurements (ie, noise), scattered radiation, and the limited spatial resolution and sampling available with PET and SPECT systems.

The kind of projection necessary for tomography is conceptually simple. If we model the internal distribution of radioactivity as a matrix of numbers such as that shown in Figure 6, then the 0° projection is found by summing along rays corresponding to columns. The 90° projection is found by summing along rows. Projections at other angles are found by rotating the parallel rays to those angles and adding the count values along the rays.

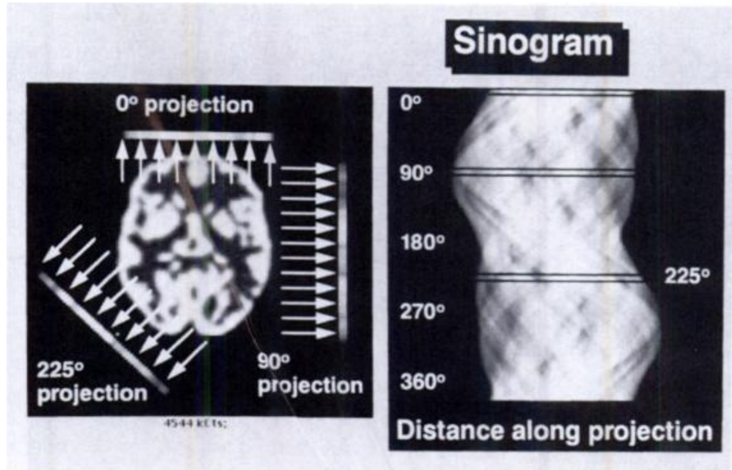

Figure 7. Projections and sinogram. Image on the left shows the internal distribution of radioactivity in a computer-simulated brain section with the calculated true projections of that section at 0°, 90°, and 225°. Image on the right shows a complete stack of the calculated projections collected at every 3°, ordered by angle. This type of display is called a sinogram. The first projection (the 0° projection) is placed in the first row of the sinogram. The next projection, which is taken at 3°, is placed in the second row, and so on.

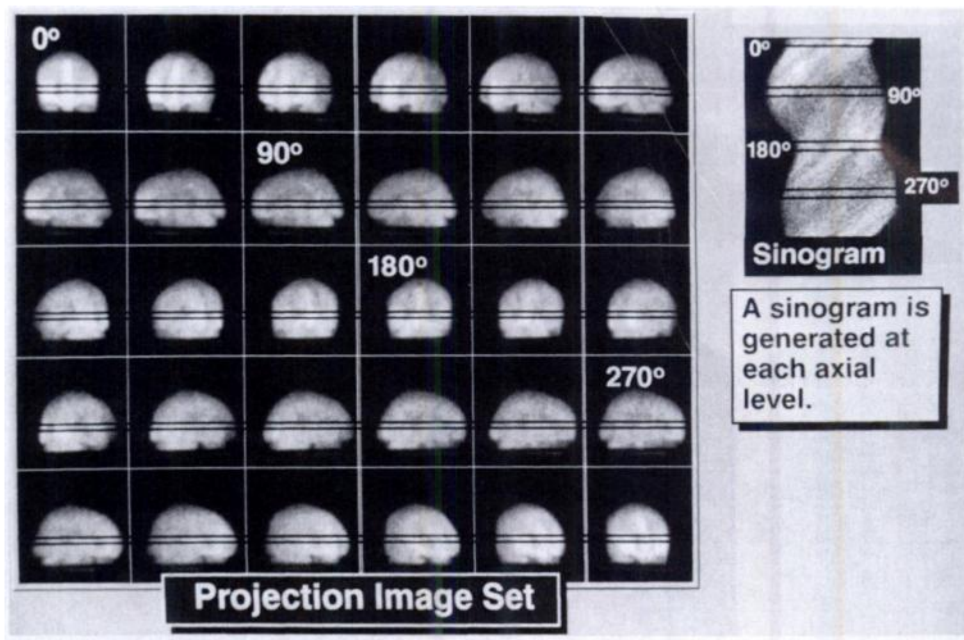

Figure 8. Real data sinogram. Scintigraphic images acquired during a SPECT brain perfusion study show the brain from a large number of angles. Each row of these images corresponds to an axial plane. The sinogram for each axial plane is simply a stack of the corresponding image rows ordered by acquisition angle.

A more graphic illustration of projection is given in Figure 7 for a computer-simulated brain image along with calculated projections at selected angles. Numerous projections from many angles are needed to reconstruct a tomographic image accurately. In a patient study, these projections are collected by a SPECT or PET system and are stacked in order by angle. When the projections are displayed in this way, a characteristic sinusoidal pattern results, and the image is called a *sinogram*. The sinogram in Figure 7 includes projections taken from 360° about the brain section. Because these are true projections, only 180° need be covered, since projections from opposed angles are identical. Because of tissue attenuation, however, this is not the case for the external measurements obtained from SPECT systems. In SPECT, opposed views differ and provide useful, nonredundant information.

The creation of the sinogram of an actual SPECT study is illustrated in Figure 8 with images collected from a brain perfusion study. The projection images are collected at equal an-

0° Backprojection

0	50	100	100	50	0
0	50	100	100	50	0
0	50	100	100	50	0
0	50	100	100	50	0
0	50	100	100	50	0
0	50	100	100	50	0

0	50	100	100	50	0

0° & 90° Backprojection

0	50	100	100	50	0	0
0	50	100	100	50	0	0
200	*250*	*300*	*300*	*250*	*200*	200
300	*350*	*400*	*400*	*350*	*300*	300
0	50	100	100	50	0	0
0	50	100	100	50	0	0

0	50	100	100	50	0

Figure 9. Backprojection. Backprojection is a mathematical operation in which projection data are added to a reconstruction matrix along the ray paths from which they were collected. For example, if the first projection were acquired at 0°, each projection value would be replicated along the image columns as shown in the left matrix. The third element of the projection is 100; thus, 100 is added to each pixel along the third column. In the right matrix, the 90° projection has been added to the 0° projection. Because the 90° projection came from summing over rows, the data in each projection cell are added to the existing count in that row. The fourth element in the 90° projection is 300. Thus, 300 is added to the current value in each pixel in the fourth row. This becomes apparent if the right matrix containing the two backprojections is compared with the left matrix, which has a single backprojection.

gular intervals over 360° by a SPECT system. Because the images are matrices of numbers, with each row of the matrix corresponding to an attenuated projection from one axial plane, the sinogram corresponding to the midplane of the brain is constructed by sequentially stacking the midplane row from each projection image. The resultant sinogram contains all of the measurements needed to reconstruct one axial section. Thus, a sinogram must be generated at each level of the brain to obtain the corresponding tomographic section.

• Backprojection

There are many ways to obtain a tomographic image from the set of PET or SPECT projections, but the most commonly used method is a technique called *filtered backprojection*. As the term implies, two mathematical operations are involved: a modification of the projections, often referred to as filtering, and a reconstruction technique, known as backprojection.

Simple Backprojection.—In simple backprojection, the projection data are successively added to an empty computer image along the ray angles at which they were acquired. Because the data for the 0° projection were acquired along columns, they are added back or "backprojected" along columns (Fig 9). In a similar way, the data for the 90° projection are added back along the rows. The result of backprojecting both the 0° and 90° projections is shown in Figure 9. The process of backprojection requires that the projected data are added along exactly the same rays as they were acquired. To accomplish this, the centers of each projection must be aligned with each other and with respect to the reconstruction matrix by a number referred to as the *center of rotation*.

Figure 10 illustrates how projection data are backprojected to reconstruct a tomographic image. As the number of projections increases, more detail can be recognized in the reconstructed image. Even with a large number of projections, however, simple backprojection does not yield an accurate tomographic image. The contrast is poor, and the image has a nonuniform background, with counts distributed in areas where there should be no activity. There

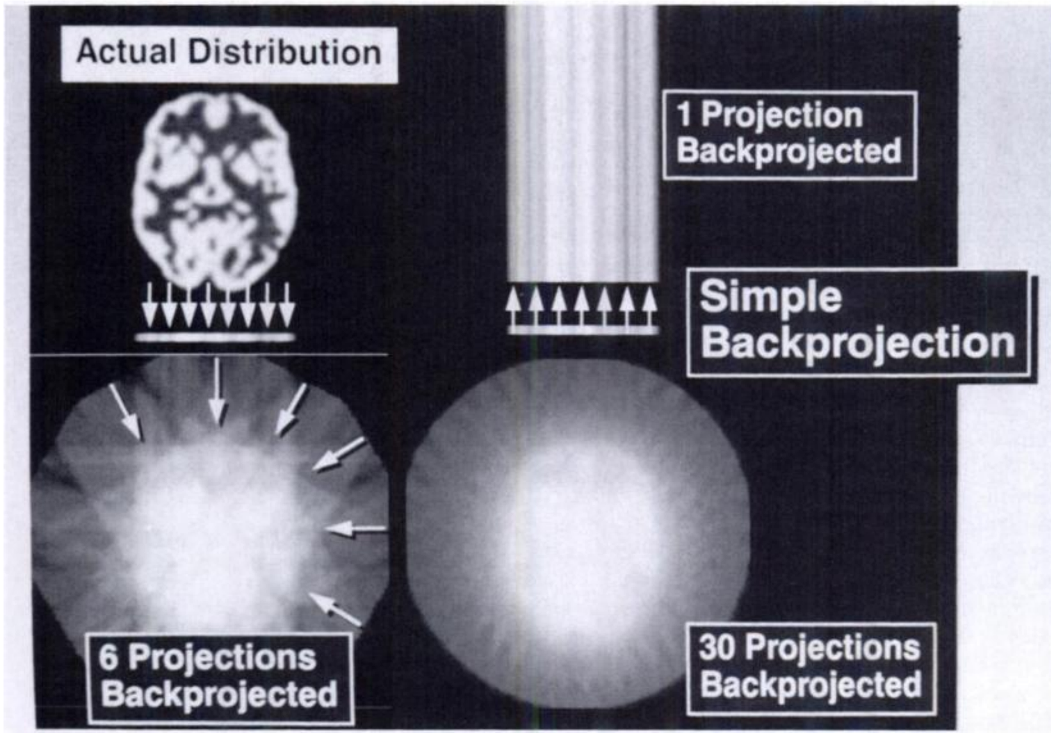

Figure 10. Simple backprojection. Image in the upper left shows the internal distribution of activity in a brain study, along with the projection at 0°. In the upper right, data from this single projection are backprojected by using the same routine described in Figure 9. Image in the lower left shows the result when the projections at 0°, 30°, 60°, 90°, 120°, and 150° are backprojected. A semblance of the actual distribution in the brain is evident. Image in the lower right shows the result after 30 backprojections. This image captures some of the features of the true internal distribution, but it is clearly not accurate.

are several ways to correct this problem, but the most efficient method is to modify the projection data in a special way (ie, through filtering) before backprojection is performed.

Filtered Backprojection.—To achieve ideal projection data, the projections must be modified through a process called *reconstruction filtering*. This process was first discovered in 1917 by Radon and was rediscovered in the 1970s when medical tomographic imaging devices were introduced (8). In reconstruction filtering, each projection is subjected to a mathematical operation called a *Fourier transform*, which restructures the projection data in terms of spatial frequency components (Fig 11). (In the remainder of the article, the word frequency refers to spatial frequency, which has units of cycles per centimeter.) The transformed projection is then multiplied by a set of numbers (ie, the reconstruction filter) that increases linearly with frequency. Because of its shape, this filter is often referred to as a ramp filter. The result is transformed back as the filtered projection. The same process is used for every projection.

There are two good reasons for using a Fourier transform to perform the projection filtering (12,13). The first reason is computational efficiency. Filtering in the frequency domain is done by multiplication. One can achieve the same results without venturing into the frequency domain, but then filtering requires a more complicated, less efficient process known as convolution. A second reason for filtering in the frequency domain is noise identification.

Figure 12 illustrates the concept of a Fourier transform. Any projection from any object can be equivalently represented as an infinite sum of sine and cosine functions of different fre-

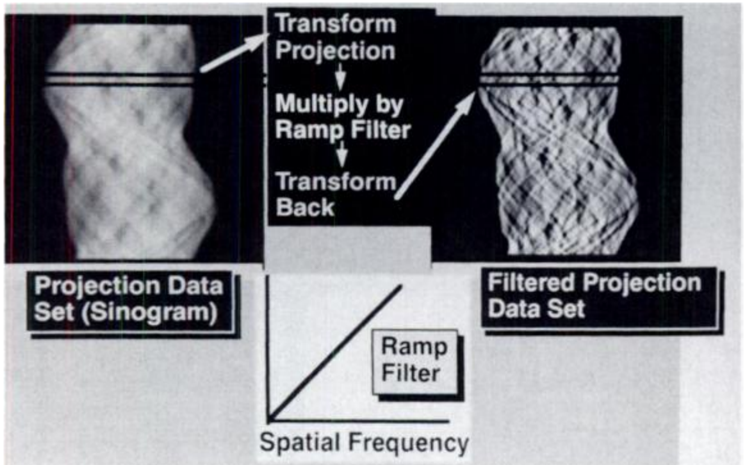

Figures 11. Filtered backprojections. The entire set of projections (left sinogram) is modified by the reconstruction filter before backprojection is performed. Each projection is transformed into the frequency domain and is multiplied by a ramp reconstruction filter. The filtered projections are then transformed back into the spatial domain where they are backprojected to obtain the tomographic image (right image).

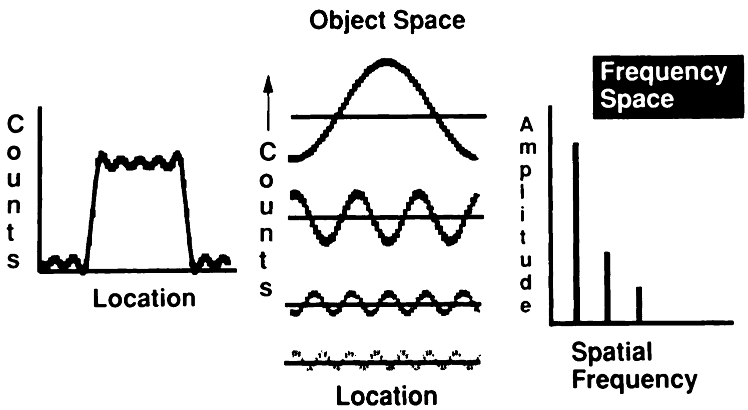

Figure 12. Fourier components. A Fourier transform takes information as it is usually represented in the spatial domain and finds the spectral components in the frequency domain. This procedure works because projections, as with most physical functions, can be equivalently represented by an infinite sum of sinusoidal functions (the Fourier series). The Fourier transform finds both the amplitude and phase associated with each sinusoidal component. This process is illustrated for the simple function shown on the left, which was synthesized by adding the four sine functions shown in the center. In this case, the spatial frequency spectrum of the result is four spikes (plot on the right). Each spike is located along the abscissa at the appropriate frequency, and the height of the spike corresponds to the amplitude of the sinusoid at that frequency.

quencies. A Fourier transform finds both the amplitudes associated with these sinusoids and the starting points in the cycles (ie, the phases). The Fourier transform takes the projection from its original representation in what is referred to as the spatial domain and finds its spectral components in the frequency domain. Although Figure 12 is a very simple, contrived example, it illustrates some features that are generally true. The general shape of a projection is derived from the low-frequency component that has a large amplitude. The sharp edges and detail are the result of the higher-frequency components, which have a small amplitude.

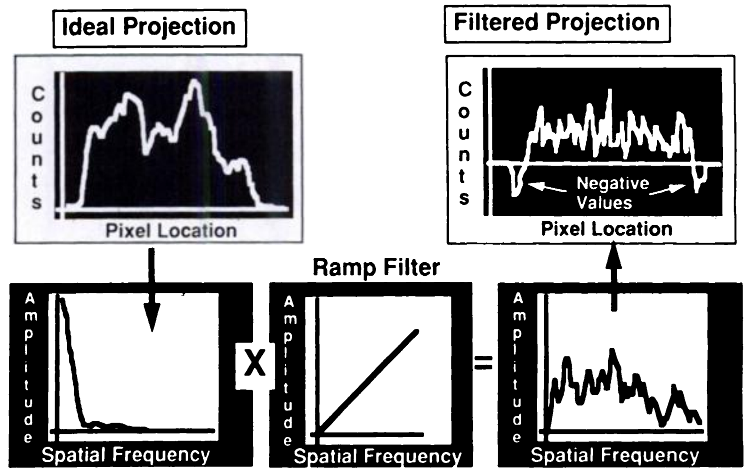

Figure 13. Filtered projections. Diagrams show the steps involved in modifying the projection data before reconstruction. At the top left is a plot of one of the projections from the sinogram. Its Fourier transform is shown below it. As in the simple example in Figure 12, the amplitude falls rapidly as the spatial frequency increases. Reconstruction filtering occurs in the frequency domain when the Fourier transform of the projection is multiplied by the ramp filter. This operation amplifies the high-frequency amplitudes with respect to the low frequencies. The result is transformed back into the spatial domain to obtain the filtered projection. Note that the process of filtering has introduced negative values into the projection.

Figure 13 shows a graphic representation of what happens with projection filtering. The spectral components of the projection data are obtained by means of applying the Fourier transform. The transformed data are multiplied by a ramp reconstruction filter, which suppresses low-frequency components and amplifies the high-frequency components. The result is then transformed back as the filtered projection. In addition to changing the shape of the projection, the application of the ramp filter introduces negative values into the filtered projection.

Windowed Reconstruction Filters.—The filtering process alters the projection data in just the right way so that when they are backprojected, the true contrast is recovered, all of the extraneous background disappears, and an accurate tomographic image is achieved (Fig 14). The preceding scenario is possible with ideal projection data; however, in the real world, all projection data are subject to noise or statistical fluctuations, which are fundamental to the imaging of radionuclides. The precision or relative level of noise in the projection data depends on the count density (counts/cm^2). This dependence is shown in Figure 15, which shows projection images of a resolution phantom acquired at increasing count densities. Although noise affects image quality throughout the entire spatial frequency range, its biggest effect is on the fine-detail portions of the image that correspond to high spatial frequency. As the noise level increases (ie, decreasing counts in Fig 15), more and more of the resolution pattern is obscured, and the portions with the finest detail disappear first. If a ramp filter is applied to noisy projections, the amplification of the noise-dominant high spatial frequencies will seriously compromise the reconstructed image.

One way of solving this problem is to remove the high-frequency components by setting them to zero. This can be done conveniently in the frequency domain by multiplying the transformed projection by a low-pass filter (Fig 16). As the name implies, the low-pass filters let the low-frequency amplitudes pass

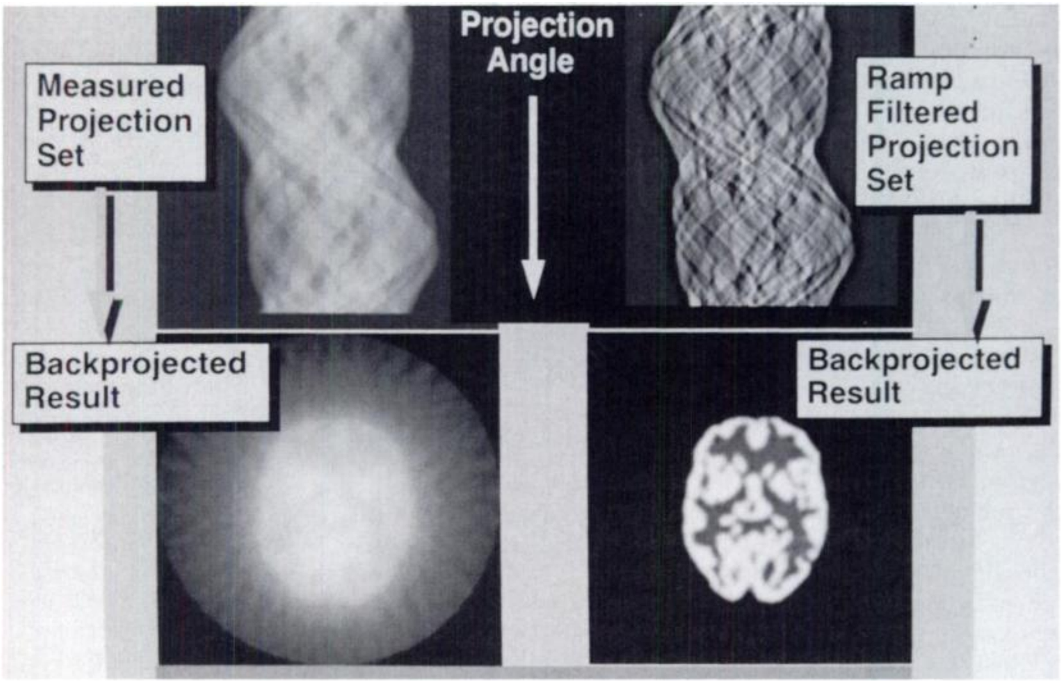

Figure 14. Comparison between simple backprojection and filtered backprojection of an ideal projection set. Simple backprojection yields an image with some of the details of the internal distribution of radioactivity, but the contrast is poor and there is a large, nonuniform background across the image. Filtered backprojection yields an accurate reconstruction for a complete projection set.

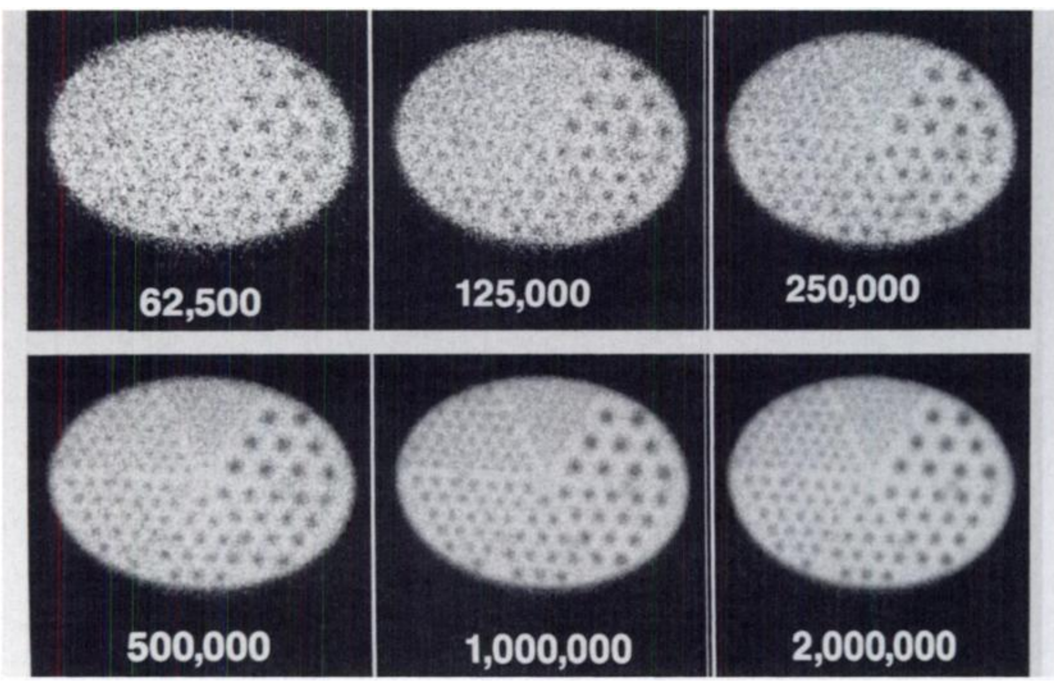

Figure 15. Image noise. Because all emission data have statistical fluctuations (noise), the precision of the data depends on the number of acquired counts. In the planar images of a resolution phantom acquired at different count densities, the sectors containing the patterns with the smallest holes are the most obscured as the count level drops. Noise dominates the small high-frequency components of the images.

through essentially unaltered, while the high frequencies are cut off (ie, set to zero). This process smooths the projection. The ramp and the low-pass filters can be combined to form a windowed reconstruction filter. A wide variety of low-pass filters exist, and many of them have been used for both SPECT and PET reconstruction. They differ mainly in how the filter falls to zero. Most low-pass filters have an adjustable parameter, which allows the user to select the frequency at which the filter will be cut off. Projection data with a high noise level require much smoothing and, therefore, should have a low-frequency cutoff. Projection data with low noise levels need little smoothing and should have a high-frequency cutoff.

The selection of the cutoff frequency in the windowed reconstruction filter must be done with care because the cutoff frequency can have a profound effect on the reconstructed image. The choice of a reconstruction filter must be balanced by two considerations: (*a*) preserving detail in the projections and (*b*) suppressing noise, which gets amplified by reconstruction filtering. Figure 17 shows how the image quality of a reconstructed image from a low count density study is compromised as the cutoff parameter is increased toward a higher frequency. As the cutoff frequency is increased, the ramp filter amplifies the noise-dominant high spatial frequencies, making the resulting image uninterpretable. Suppression of noise has its own disadvantages, since at the same time noise is being reduced, real detail in the projections is also being smoothed and lost. As illustrated in a reconstruction of a higher count density study (Fig 18), which has a relatively low noise level, a low cutoff frequency smooths out true detail in the reconstructed image. In addition to image count density, other factors influence the optimal choice of reconstruction filter parameters, including the size and contrast of the image, the acquisition gain (ie, the pixel size), and the spatial resolution. Although discussion of these factors is beyond the scope of this article, they are discussed in several of the references (1,2,5-7,10,12).

• Reconstruction Artifacts

The ability to reconstruct tomographic images by using filtered backprojection depends on the underlying assumptions about the projections. Typical artifacts that result from violations of these assumptions include motion, uniformity, and attenuation artifacts. In addition, errors in selection of the center of rotation, insufficient angular sampling, and errors in selection of pixel size can result in poor-quality reconstructed images.

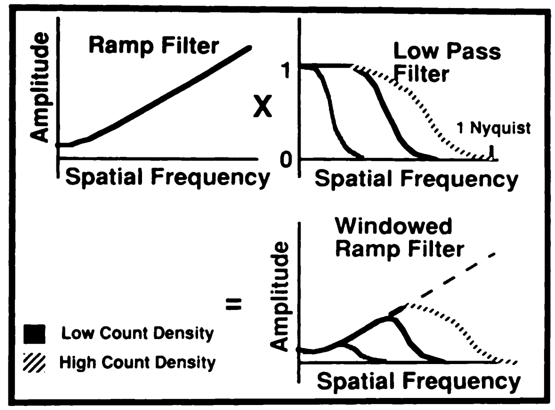

Figure 16. Reconstruction filters. The appropriate reconstruction filter for ideal projection data (ie, no noise) is the ramp. However, when the ramp filter is applied to noisy data, the noise is amplified at the expense of the useful projection data. One way to avoid this problem is to combine a smoothing or low-pass filter with the ramp reconstruction filter. This "windowed" reconstruction filter is controlled by parameters that cause the filter to fall to zero at selected frequencies. When the projections are very noisy, it is desirable to have the filter cut off at a low frequency (gray line in the plots at the right). When the statistical precision of the projection data is good, the filter should cut off at a higher frequency (broken line in the plots at the right).

Motion Artifacts.—In the reconstruction of tomographic images, there is a tacit assumption that the projections at each angle are drawn from the same distribution of radioactivity. This means that the internal distribution of radionuclides should remain static during the measurement time. Because of the low sensitivity of radionuclide images, the required imaging time may be long (5–30 minutes), which could lead to changes in the radioactivity distribution from several sources: (*a*) the kinetics of the radiopharmaceutical, (*b*) the motion of internal organs such as the heart and lungs, and (*c*) the motion of the entire patient. Of these, patient motion is probably the most important. Figure 19 shows the types of artifacts that can be encountered with patient motion. Obviously, patient motion has a profound effect on tomographic images, and steps should be taken to minimize this motion as much as possible.

Uniformity Artifacts.—Another important assumption in the reconstruction of tomographic images is that the detectors have a uniform sen-

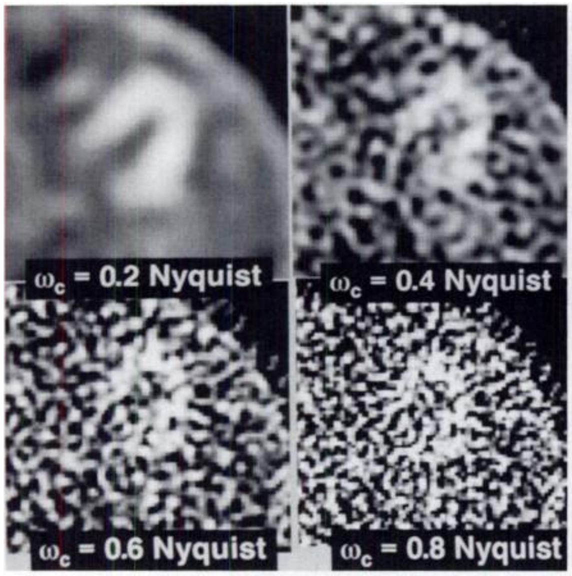

17.

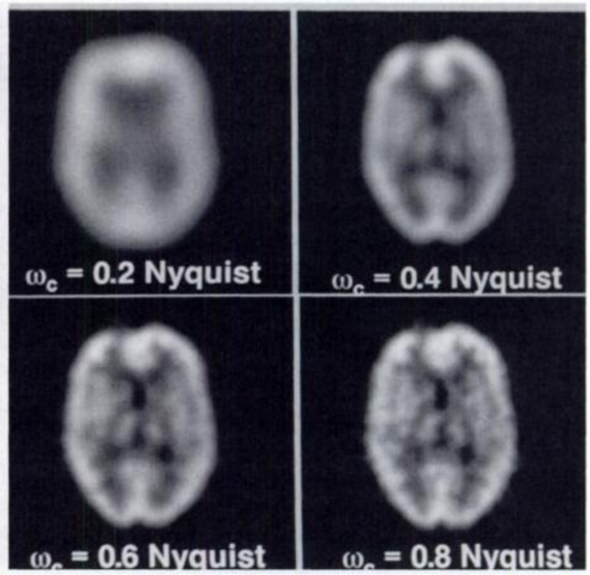

18.

Figures 17, 18. (17) Image quality as a function of filter cutoff frequency for a projection set with a low count density. Four reconstructed images of the same projection data from a Tl-201 myocardial perfusion study are shown. The cutoff frequency (ω_c) is varied from 0.2 to 0.8 Nyquist. The Nyquist frequency is the highest frequency that can be represented in sampled data, so that 0.2 Nyquist means that we are passing through about 20% of the spatial frequencies and discarding the upper 80%. Because the projection data from this study had a very high noise level (ie, low count density), a low-frequency cutoff was required. **(18)** Image quality as a function of filter cutoff frequency for a projection set with a high count density. Four reconstructed images from a high-count Tc-99m HMPAO brain perfusion study show how image quality is compromised as the cutoff frequency (ω_c) is decreased toward lower frequency and the useful detail in the image is lost by oversmoothing. (The same reconstruction filters as used in Fig 17 were used.) The best cutoff for this reconstruction probably lies somewhere between 0.6 and 0.8 Nyquist.

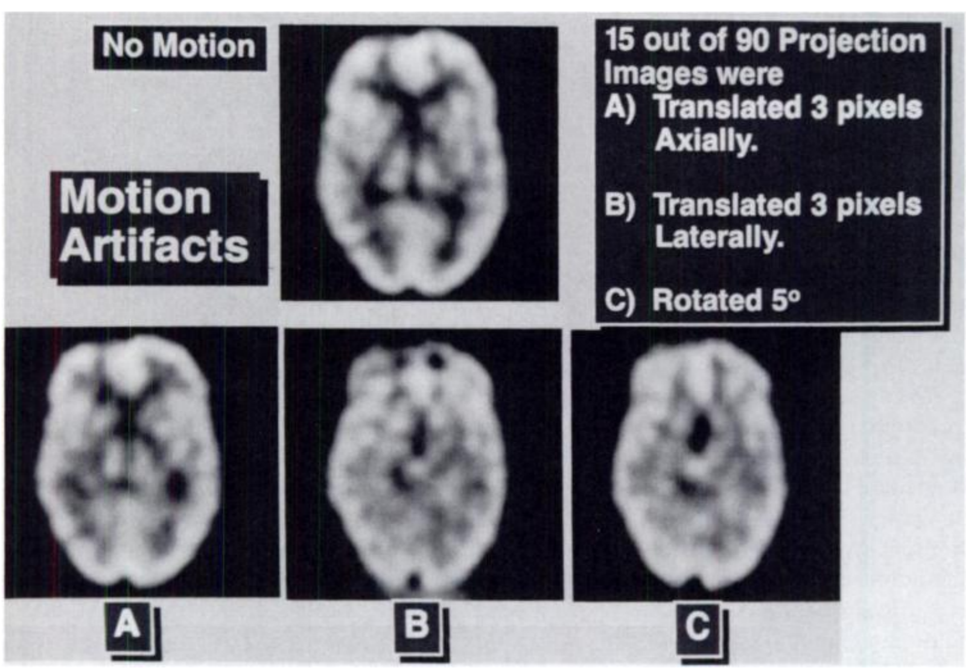

Figure 19. Motion artifacts. Image at the top was reconstructed from projections in which the patient was stable. Three images at the bottom show the results when there was patient motion axially (*A*), laterally (*B*), and rotationally (*C*). Motion in the axial direction caused subtle differences in the reconstruction; lateral and angular motion caused extreme artifacts.

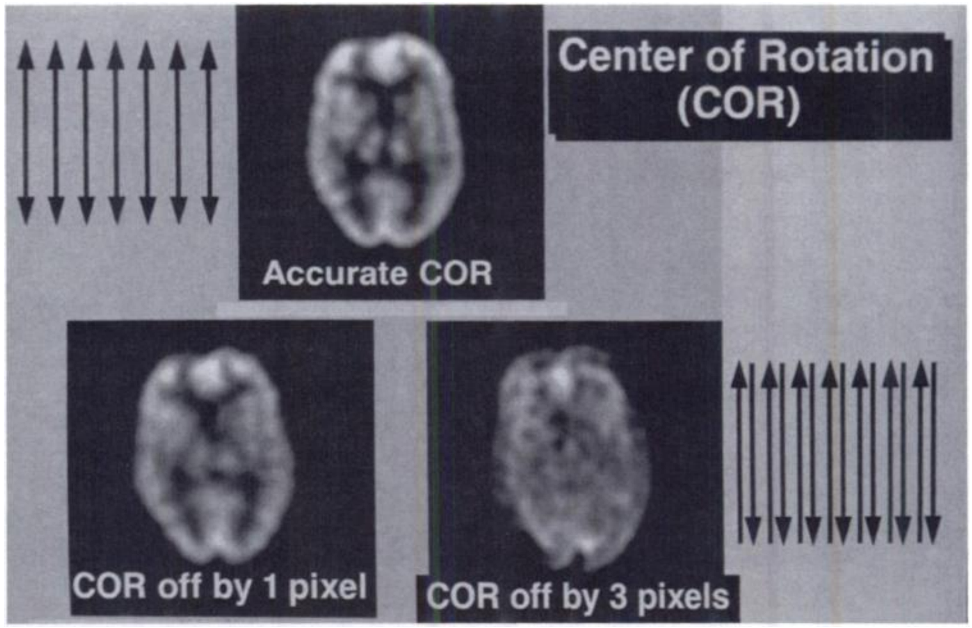

Figure 21. Center of rotation artifacts. The backprojection algorithm aligns the projections with respect to the reconstruction matrix by a number referred to as the center of rotation (*COR*). When an inaccurate center of rotation is used, the projections are not properly aligned during backprojection, and each point in the reconstruction matrix is blurred into a small ring. To avoid this problem, the center of rotation must be accurate to within at least ±0.5 pixels.

sitivity. If there are regional variations in the sensitivity of the detectors, annular artifacts will be introduced into the tomographic sections (Fig 20). Uniformity artifacts will be most extreme for large distributions of radioactivity and when the nonuniformity is close to the center of rotation. On SPECT and PET systems that meet the manufacturers' specifications, uniformity artifacts are not a problem. However, they can occur if the detectors are not properly tuned or if, in the case of SPECT, the collimators are damaged.

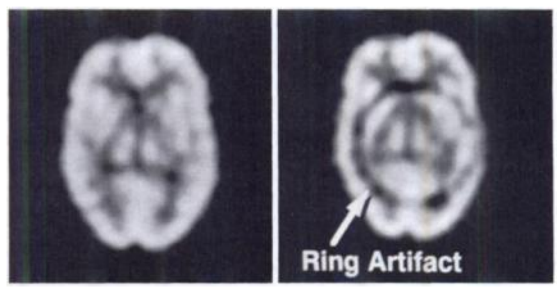

Figure 20. Uniformity artifacts. Emission CT detectors acquiring the projection data must have uniform sensitivity across the field of view. Regional variations in detector uniformity give rise to annular artifacts centered about the center of rotation. The projection data from which the right brain perfusion image was reconstructed had a 20% loss of sensitivity over a 2-cm^2 portion of the detector.

Errors in Selection of the Center of Rotation. —Tomographic systems (when properly installed) are aligned to an imaginary axis in space referred to as the axis of rotation. If a radioactive line source were positioned along the axis of rotation, its image would lie at the same x coordinate in every projection. This location is referred to as the center of rotation, and its value must be accurately known.

When the backprojection is performed with an accurate center of rotation, the rays from opposing views coincide, forming well-defined points. If the wrong center of rotation is used, the backprojected rays from opposed views miss each other, and, instead of well-defined points, small rings are formed. Losses in spatial resolution become perceivable when the error in the center of rotation is on the order of 0.5 pixels. Distortion becomes extreme when the error exceeds 1 pixel (Fig 21).

Insufficient Angular Sampling. —Tomography requires a complete projection set. The number of samples needed to make a set of pro-

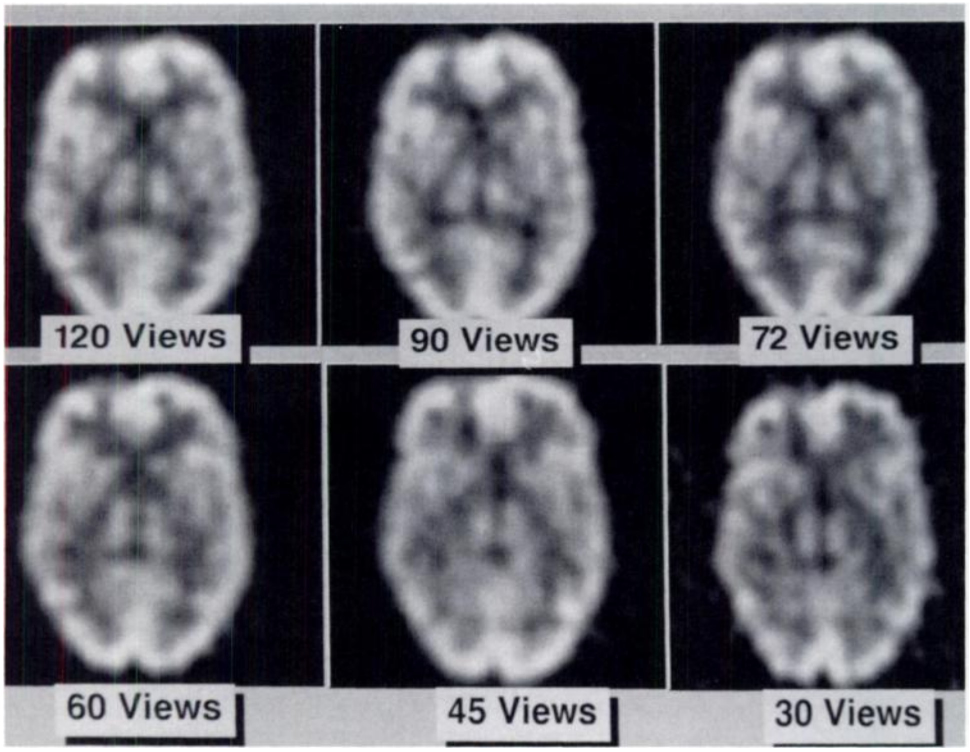

Figure 22. Image quality as a function of angular sample. A series of brain perfusion images reconstructed with 120, 90, 72, 60, 45, and 30 projection views demonstrates that as the number of projection views decreases, the reconstructed image appears to break apart, especially at the edges of the larger structures. (The sampling time was adjusted so that the total counts were the same in each study.)

jections complete depends on two factors: (*a*) the expected spatial resolution in the reconstructed section, and (*b*) the size of the radionuclide distributions. Bigger distributions require more angular samples. At each angular step, a point is sampled on the circumference of the circular field that encompasses the entire distribution. A useful rule of thumb is that the distance between these sampling points (corresponding to the angular steps) should be less than the system spatial resolution as measured by the full width at half maximum (FWHM). Typical numbers of angular samples range from 60 to 120 in SPECT and up to 512 in PET.

The effect of angular sampling is shown in Figure 22, in which reconstructed images from a brain perfusion study were acquired at different angular sampling but with the same total counts. As the angular sampling becomes insufficient, the reconstructed images appear to break apart, especially at the edges of the larger structures, and streak and star artifacts are produced.

Errors in Selection of Pixel Size.—The projection data collected on SPECT and PET systems are sampled into a computer matrix. This digitization can cause a loss of resolution if the image matrix is too coarse. The pixel size of the matrix should be selected so that it does not substantially alter the system resolution. As a rule of thumb, the pixel size should be less than one-half of the system FWHM. For example, if the resolution in the reconstructed image is 12 mm, the pixel size should be less than 6 mm.

The effect that digital sampling has on tomographic sections is seen in Figure 23, in which reconstructed images of the brain acquired at different pixel sizes are shown. As the pixel size approaches the FWHM, there is substantial degradation in the quality of the reconstructed image.

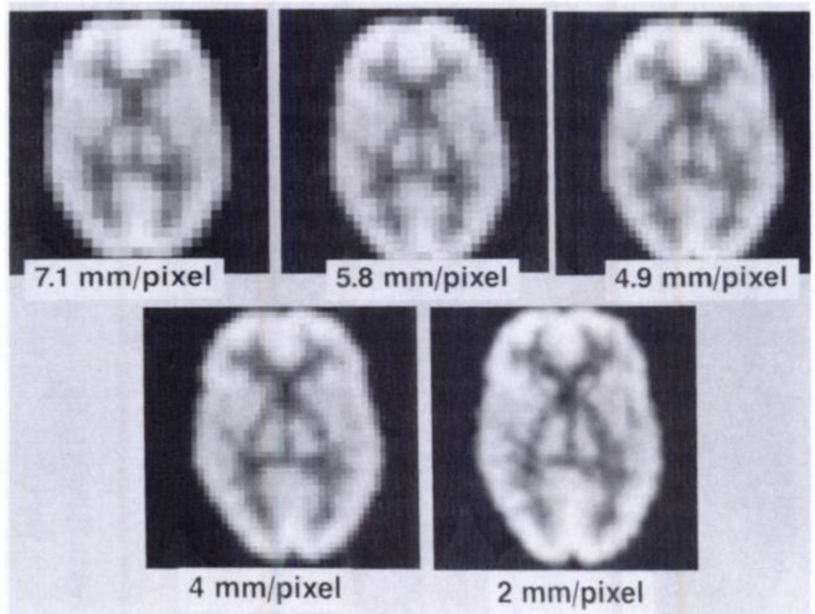

Figure 23. Image quality as a function of pixel size. A series of brain perfusion images reconstructed with projection views of 7.1–2 mm per pixel demonstrates that the quality of the reconstructed image decreases as the pixel size becomes the dominant factor in determining the system resolution. (The system FWHM was 10 mm for the image with 2 mm pixels.)

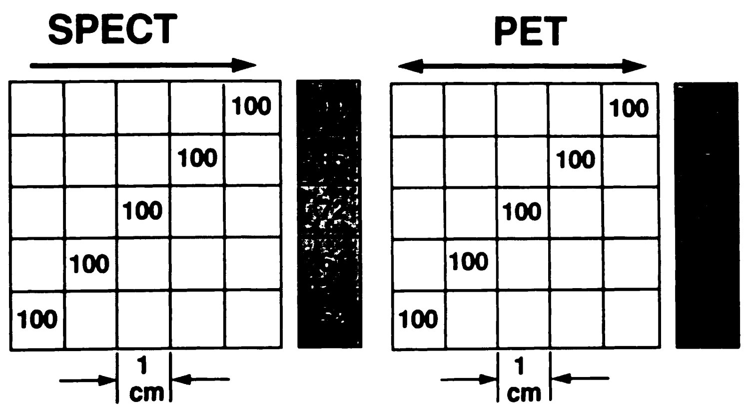

Figure 24. Attenuation in SPECT and PET. Diagram on the left shows how SPECT projection data depend on the source location. Apparent radioactivity that is detected becomes progressively smaller as the amount of tissue between the source and the detector increases. Diagram on the right shows the effect of attenuation on PET projection data. In PET, the decrease in detected radioactivity depends on the total path length through the object determined by the coincidence detectors. Thus, location of the source along a ray does not affect the amount of attenuation. To obtain true tomographic images, corrections for attenuation must be applied for both PET and SPECT projections.

Attenuation Artifacts.—Because of attenuation, the information gathered by PET or SPECT systems does not represent the true projection data necessary for accurate tomography (Fig 24). The problem is somewhat more extreme for SPECT, since the effect of attenuation depends on the source location. Corrections for attenuation are necessary to obtain true tomographic images in both PET and SPECT. The correction for PET depends only on the total path length through the body.

Figure 25 illustrates the effect of an attenuation artifact in a Tl-201 myocardial perfusion study. Such artifacts in uncorrected studies could be mistaken for disease.

■ CONCLUSION

Emission CT offers a three-dimensional window into the internal distributions of radionuclides. However, it depends on several fundamental

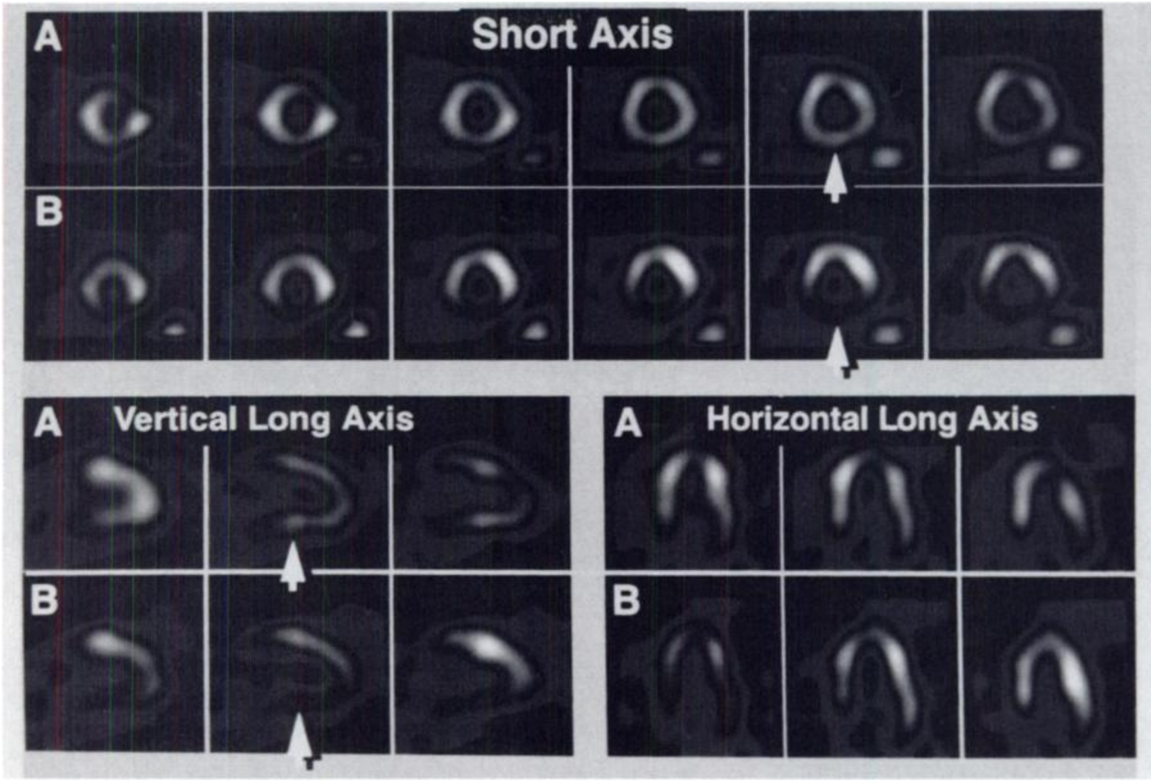

Figure 25. Attenuation artifacts. Images demonstrate a common attenuation problem in myocardial perfusion SPECT. A set of Tl-201 images corrected for attenuation (*A*) are shown with the corresponding uncorrected images (*B*). There is an artifactual decrease in the activity of the inferior wall of the heart (arrows) in the uncorrected images that could easily be mistaken for coronary artery disease.

principles that are critical to the production of useful, diagnostic information. To obtain accurate tomographic images requires both good projection data and the intelligent selection of reconstruction filters.

■ REFERENCES

1. Brooks RA, DiChiro G. Theory of image reconstruction in computed tomography. Radiology 1975; 117:561-572.
2. Ell PJ, Holman BL. Computed emission tomography. New York, NY: University Press, 1982.
3. Ter-Pogossian MM. The origins of positron emission tomography. Semin Nucl Med 1992; 22:140-149.
4. Budinger TF. Physical attributes of single photon tomography. J Nucl Med 1980; 21:579-592.
5. Parker JA. Quantitative SPECT: basic theoretical considerations. Semin Nucl Med 1989; 19: 3-12.
6. Blokland AK, Reiber HC, Pauwels EKJ. Quantitative analysis in single photon emission tomography. Eur J Nucl Med 1992; 19:47-61.
7. Tsui BMW, Xide Z, Frey EC, McCartney WH. Quantitative single photon emission computed tomography: basics and clinical considerations. Semin Nucl Med 1994; 24:38-65.
8. Webb S. From the watching of shadows: the origins of radiological tomography. New York, NY: Oxford Medical, 1990.
9. Heller SL, Goodwin PN. SPECT instrumentation: performance, lesion detection, and recent innovations. Semin Nucl Med 1987; 17:184-199.
10. Muehllehner G, Karp JS. Positron emission tomography: technical considerations. Semin Nucl Med 1986; 16:35-50.
11. Koeppe RA, Hutchins GD. Instrumentation for positron emission tomography: tomographs and data processing and display systems. Semin Nucl Med 1992; 22:162-181.
12. Miller TR, Sampathkumaran KS. Digital filtering in nuclear medicine. J Nucl Med 1982; 23: 66-72.
13. Bracewell RN. The Fourier transform and its applications. 2nd ed. New York, NY: McGraw Hill, 1965.

This article meets the criteria for 1.0 credit hour in Category 1 of the AMA Physician's Redognition Award. To obtain credit, see the questionnaire on pp 919-922.